

Reinhard Schweitzer-Stenner<sup>1,2</sup>

Fatma Eker<sup>3</sup>

Alejandro Perez<sup>1</sup>

Kai Griebenow<sup>1</sup>

Xiaolin Cao<sup>4</sup>

Laurence A. Nafie<sup>4</sup>

<sup>1</sup> Department of Chemistry,  
University of Puerto Rico,  
Río Piedras Campus,  
San Juan,  
Puerto Rico 00931

<sup>2</sup> Department of Chemistry,  
Drexel University,  
Philadelphia, PA 19104

<sup>3</sup> Department of Biology,  
University of Puerto Rico,  
Río Piedras Campus,  
San Juan,  
Puerto Rico 00931

<sup>4</sup> Department of Chemistry,  
Syracuse University,  
Syracuse, Syracuse,  
NY 13244

Received 15 June 2003;  
accepted 18 July 2003

# The Structure of Tri-Proline in Water Probed by Polarized Raman, Fourier Transform Infrared, Vibrational Circular Dichroism, and Electric Ultraviolet Circular Dichroism Spectroscopy

**Abstract:** Tripeptides serve as model systems for understanding the so-called random-coil state of peptides and proteins. While it is well known that polyproline or proline-rich polypeptides adopt the very regular polyproline-II (PPII) or left-handed  $3_1$ -helix conformation, it was thus far not clear whether this is also the predominant structure adopted by proline-containing tripeptides. To clarify this issue, we have investigated the amide I' band profile in the ir, isotropic, and anisotropic Raman, and vibrational circular dichroism (VCD) spectrum of cationic and zwitterionic tri-proline in  $D_2O$ . The data were analyzed by modifying a recently developed algorithm, which allows one to obtain the central dihedral angles of tripeptides from the amide I' band intensities (R. Schweitzer-Stenner, *Biophysical Journal*, 2002, Vol. 83, pp. 523–532). Our analysis revealed that the peptide adopts a nearly canonical PPII structure in water with  $\psi$  and  $\phi$  values in the range of  $175^\circ$ – $165^\circ$  and  $-70^\circ$ – $(-80^\circ)$ , respectively. This is fully confirmed by the respective electronic ultraviolet-CD

Correspondence to: Reinhard Schweitzer-Stenner; email: RSchweitzer-Stenner@drexel.edu

Contract grant sponsor: Center for Research in Protein Structure, Function and Dynamics (CRPSFD), NIH-SCORE, and Fondos Institucionales para la Investigación of the University of Puerto Rico (UPR)

Contract grant number: P20 RR16439-01 (NIH-COBRE II, CRPSFD), S06 GM008102-3052 (NIH-SCORE), and 20-02-2-78-514 (UPR)

*Biopolymers* (Peptide Science), Vol. 71, 558–568 (2003)

© 2003 Wiley Periodicals, Inc.

spectra. Our result indicates that the strong PPII propensity of *trans* proline results from local interactions between the pyrrolidine ring and the backbone and is not due to any long-range interactions. © 2003 Wiley Periodicals, Inc. Biopolymers (Pept Sci) 71: 558–568, 2003

**Keywords:** *tripeptides; random-coil state; proteins; polyproline; proline-containing tripeptides; amide I'*

## INTRODUCTION

For a long period of time it has been believed that the unfolded state of proteins and peptides is structurally completely disordered, because the respective dihedral angles can, in principle, sample the entire allowed region of the Ramachandran space. This view was theoretically corroborated by the random coil model introduced by Brant and Flory,<sup>1</sup> who argued that an unfolded polypeptide could be treated like a synthetic flexible polymer. During the last fifteen years, however, this notion has been substantially modified in that it was recognized that in many cases some residual native and non-native structure persists.<sup>2</sup> In this context the polyproline II conformation has emerged as one of the structural motifs in the disordered state of peptide fragments as well as of proteins.<sup>2,3</sup> The canonical type II polyproline (PPII) is a left-handed helix with an axial translation of 3.2 Å composed of three prolyl residues per turn.<sup>4</sup> Based on the similarity of electronic ultraviolet CD (ECD) spectra, Tiffany and Krimm suggested 35 years ago that this conformation is not only adopted by polyproline but contributes also to the coil state of polylysine and polyglutamic acid.<sup>5,6</sup> This view was later confirmed by vibrational circular dichroism spectroscopy (VCD).<sup>7,8</sup> PPII segments have been identified in the x-ray structure of many proteins<sup>9</sup> and CD and NMR data indicate that it is adopted by a variety of cell receptor binding peptides.<sup>3,10</sup> Based on Raman optical activity measurements Barron and co-workers have hypothesized that for some proteins PPII may constitute an intermediate state in the process of amyloid fibril formation.<sup>11</sup>

While classical secondary structures like helices,  $\beta$ -sheets, and turns are stabilized by a combination of local, nonlocal and peptide–solvent interactions, it is generally thought that the PPII conformation of non-proline residues can exist only in water and reflects the local propensity of a given residue.<sup>12,13,14,15</sup> From this it follows that even short peptides should be able to adopt the PPII conformation, in contrast to the common belief that their structure is completely random.<sup>16</sup> Indeed, a (temperature-dependent) mixture of PPII and extended  $\beta$ -strand conformation have been obtained for the tri-alanine<sup>17,18,19</sup> and various alanine-based oligopeptides.<sup>20,21</sup> Even the classical alanine dipeptide seems to be predominantly PPII.<sup>13</sup>

On the contrary, tri-valine mostly adopts an extended  $\beta$ -sheet conformation.<sup>17,18</sup> First measurements on different AXA peptides indicate that most side chains fluctuate between PPII and  $\beta$ -strand in the absence of nonlocal interactions (Eker, Cao, Nafie, Schweitzer-Stenner, unpublished results). The respective molar fractions most likely reflect side chain–solvent and side chain–backbone interactions.<sup>15</sup>

It is surprising that even though PPII has become an important issue for the structure analysis of even short peptides, the solution structure of tri-proline has not yet been determined. The above-cited results clearly lead to the prediction that it should adopt a structure close to the canonical PPII. Dukor and Keiderling reported VCD spectra of a series of  $(P)_n$  peptides including  $P_3$  and interpreted their result as indicating a PPII structure.<sup>8</sup> Helbecque and Louchoux–Lefebvre used electronic ECD to investigate a series of  $GP_n$  peptides and found that  $n=3$  is the minimal number of proline residues required to obtain a PPII signal.<sup>22</sup> None of these studies ruled out an admixture of other conformations. To our best knowledge the dihedral angles of  $P_3$  have not yet been determined. In the present study we measured and analyzed the amide I' band in the FTIR, polarized Raman, and VCD spectra of tri-proline to fill this gap. To obtain the dihedral angle between the two peptide groups from the amide I'' band profiles in these spectra, we employed a modified and mathematically more consistent version of a recently developed algorithm.<sup>23</sup> Our results were checked by measuring the ECD signal in the far-uv region.

## THEORETICAL BACKGROUND

The theory used to obtain the dihedral angles of tripeptides from the amide I' bands in their visible Raman and ir spectra has been described in detail elsewhere.<sup>23</sup> In what follows, this theory will be briefly reviewed and slightly modified to extend its applicability. We assume a two-oscillator model to describe the mixing between the two amide I' modes of tripeptides by transition dipole and through bond coupling.<sup>24</sup> The corresponding excitonic states are written as

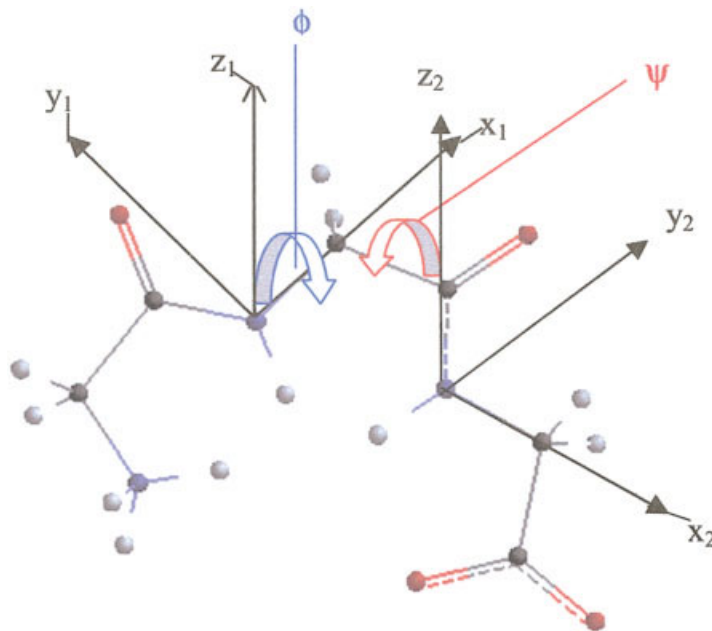


**FIGURE 1** Reference structure of a tripeptide ( $\phi=180^\circ$ ,  $\psi=0^\circ$ , tri-glycine has been chosen for the sake of simplicity) and representation of the coordinate system chosen for the transformation of the Raman tensor and the transition dipole moment. The structure was obtained by using the program TITAN from Wavefunction, Inc.

$$|\chi_{-}\rangle = \cos\nu|\chi_{1}\rangle - \sin\nu|\chi_{2}\rangle \quad (1)$$

$$|\chi_{+}\rangle = \sin\nu|\chi_{1}\rangle + \cos\nu|\chi_{2}\rangle$$

The parameter  $\nu$  describes the degree of mixing between the unperturbed states  $|\chi_{1}\rangle$  and  $|\chi_{2}\rangle$ , which is maximal for  $\nu=45^\circ$ . This requires the unperturbed modes to be accidentally degenerate.  $|\chi_{+}\rangle$  and  $|\chi_{-}\rangle$  are the excitonic states of the in-phase (ip) and out-of-phase (oop) combination of the interacting modes.

The mixing parameter  $\nu$  can be determined from the intensity ratio  $R_{\text{iso}} = I_{\text{iso}}^{-} / I_{\text{iso}}^{+}$  of the two amide I' bands in the spectrum of isotropic Raman scattering ( $I_{\text{iso}}^{-}$  and  $I_{\text{iso}}^{+}$  are the isotropic intensities of  $|\chi_{-}\rangle$  and  $|\chi_{+}\rangle$ ) by utilizing the equation:

$$\nu = \frac{1}{2} \arcsin\left(\frac{1 - R_{\text{iso}}}{1 + R_{\text{iso}}}\right) \quad (2)$$

The corresponding ratio  $R_{\text{aniso}} = I_{\text{aniso}}^{-} / I_{\text{aniso}}^{+}$  depends on the mixing ratio and on the dihedral angles  $\phi$  and  $\psi$ , which determine the relative orientation of the two peptide groups. In order to extract this information from the experimentally determined  $R_{\text{aniso}}$  value, one has to calculate the Raman tensor of the excitonic states  $|\chi_{-}\rangle$  and  $|\chi_{+}\rangle$ :

$$\hat{\alpha}_{-} = \cos\nu \cdot \hat{\alpha}_{1} - \sin\nu \cdot \hat{\alpha}_{2} \quad (3)$$

$$\hat{\alpha}_{+} = \sin\nu \cdot \hat{\alpha}_{1} + \cos\nu \cdot \hat{\alpha}_{2}$$

where  $\hat{\alpha}_{1}$  and  $\hat{\alpha}_{2}$  are the amide I' Raman tensors of the two peptide groups. In order to calculate  $\hat{\alpha}_{1}$  and  $\hat{\alpha}_{2}$  one has to transform one peptide tensor into the coordinate system of the other one. Thus, the Raman tensors of the excitonic states become dependent on the relative orientation of the peptide groups. In our earlier study this coordinate transformation was achieved by rotating the coordinate system of  $\hat{\alpha}_{1}$  by the tilt angle  $\theta$  between the peptide normals (i.e., the  $z$  axes in Figure 1) and subsequently by an angle  $\eta$ , which is the azimuthal angle between the now coplanar peptide groups (i.e., between the carbonyl groups of the peptides in a planar conformation, cf. Figure 1).<sup>23</sup> While this procedure is in principle correct, it has the disadvantage that the real value for  $\eta$  depends on the choice of the coordinate system for the rotation around  $\theta$ . Thus, it is conformationally dependent and cannot generally be identified with the angle between the peptide groups in a coplanar configuration, as done in Ref. 23. Moreover, this procedure makes the selection of the coordinate system for the Raman tensor dependent of the actual dihedral angles  $\phi$  and  $\psi$ . This is problematic because it obfuscates the orientation of the coordinate system of the Raman tensor with respect to the principal axes of the Raman tensor

(PART). Even though a check yielded a negligible small error for the earlier investigated tripeptides,<sup>17</sup> it is preferable to use a more rigorous formalism, which can be obtained by using the coordinate systems in Figure 1 (this coordinate system was also used in Ref. 23, but not for the rotation of the Raman tensor, in contrast to what is stated in the article). The  $x$  axis of the coordinate system coincides with the  $\text{NC}_\alpha$  bonds of the two peptides and thus with the rotational axis of the dihedral angle  $\phi$ . The tensor  $\hat{\alpha}_2$  can be rotated from  $S_1(x_1, y_1, z_1)$  into  $S_2(x_1, y_1, z_1)$  by the matrix operation:

$$\hat{\alpha}_2(S_1) = R^T(\omega)(R^T(\psi)[(R^T(\xi) \times [(R^T(\phi')\hat{\alpha}_2(S_2)R(\phi'))R(\xi)]]R(\psi))R(\omega) \quad (4)$$

which can be understood as follows. First,  $S_1$  has to be rotated by an angle  $\phi' = \phi - \pi$ . Subsequently, a rotation by  $x$  in the  $xy$  plane is necessary so that the  $y$  coordinate coincides with the  $\text{C}_\alpha\text{C}$  bond, which is the rotational axis for  $y$ .  $\xi$  is the angle formed by the  $y_1$  axis and the  $\text{C}_\alpha\text{C}$  bond. Next, the system is rotated by the dihedral angle  $\psi$ . The fourth step involves the rotation by an angle  $\omega$ , which is formed by the  $\text{C}_\alpha\text{C}$  bond and the  $y_2$  axis. This causes the abscissa to coincide with the  $\text{NC}_\alpha$  bond. This rotation causes the  $y$  axis to coincide with the  $\text{NC}_\alpha$  bond. Note that for a coplanar arrangement of the peptide groups as depicted in Figure 1,  $\omega$  and  $\xi$  can be obtained from textbooks on peptide structure with  $96^\circ$  and  $20^\circ$ , respectively).

The tensors calculated by means of Eqs. (3) and (4) can be used to calculate the isotropic and anisotropic scattering for the two excitonic states:

$$\begin{aligned} \beta_{s\pm}^2 = \frac{1}{9} (\text{Tr } \hat{\alpha}_\pm)^2 \gamma_{\text{aniso}\pm}^2 = \frac{1}{2} [(\alpha_{xx,\pm} - \alpha_{yy,\pm})^2 \\ + (\alpha_{yy,\pm} - \alpha_{zz,\pm})^2 + (\alpha_{zz,\pm} - \alpha_{xx,\pm})^2] \\ + \frac{3}{4} [(\alpha_{xy,\pm} + \alpha_{yx,\pm})^2 + (\alpha_{yz,\pm} + \alpha_{zy,\pm})^2 \\ + (\alpha_{zx,\pm} + \alpha_{xz,\pm})^2] \end{aligned} \quad (5)$$

Eq. (5) can be used to calculate  $R_{\text{iso}} = \beta_{s-}/\beta_{s+}$  and  $R_{\text{aniso}} = \gamma_{\text{aniso}-}/\gamma_{\text{aniso}+}$  as function of the mixing parameters  $\nu$  and the dihedral angles  $\phi$  and  $\psi$ .

In the next step we use the mixing parameter and the intensity ratio  $R_{\text{IR}} = I_{\text{IR}}^-/I_{\text{IR}}^+$  in the FTIR spectrum to obtain the angle  $\tilde{\theta}$  between the transition dipole moments of the amide I' mode. The  $\tilde{\theta}$  can be calculated as function of  $\phi$  and  $\psi$ . The related algorithm is described in Ref. 23. Only those  $\phi$  and  $\psi$  values that reproduce the experimentally obtained  $R_{\text{aniso}}$  and  $R_{\text{IR}}$

are considered consistent with the experimental data. Thus, one generally obtains up to eight solutions. In most cases six of them can be ruled out because they represent sterically forbidden conformations.

The physical, dihedral, and oriental parameters thus obtained were finally used to simulate the VCD signal of amide I' as described in detail earlier.<sup>17</sup> Thus, VCD serves a check of our analysis and is used to discriminate between the different solutions obtained from the ir and Raman data. Generally, this procedure yields a single pair of values for  $\phi$  and  $\psi$ .

## MATERIAL AND METHODS

### Materials

L-prolyl-L-alanine and L-prolyl-L-prolyl-L-proline were purchased from Bachem Bioscience, Inc. (>98% purity), and used without further purification.  $\text{NaClO}_4$  and the quencher KI were obtained from Sigma-Aldrich Chemical Company (St. Louis, MO). All chemicals were of analytical grade. The peptides were dissolved in  $\text{D}_2\text{O}$  at concentrations of 0.15M (for ir and Raman), 0.075M (VCD) and 1 mM (ECD). The pD of the solutions were adjusted by adding small aliquots of DCl or NaOD, respectively, to obtain the cationic, zwitterionic, and anionic state of the peptides. The pD values were determined by utilizing the method of Glasoe and Long<sup>25</sup> to correct the values obtained from pH electrode measurements. For the Raman experiments the solvent contained 0.25–0.1M  $\text{NaClO}_4$  whose  $934 \text{ cm}^{-1}$  Raman band was used as an internal standard.<sup>26</sup> Additionally, we added 20  $\mu\text{L}$  of KI M of in order to partially quench the fluorescence of the tri-proline samples.

### Methods

**Raman Spectroscopy.** The 442 nm excitation (70 mW) was obtained from a HeCd laser (Model IK 4601R-E, Kimmon Electric US). The polarized exciting laser beam was focused onto the sample with a lens of 100 mm focal length. The Raman scattered light was collected in a  $135^\circ$  back-scattering geometry. The scattered radiation was imaged onto the entrance slit (width adjusted to 100  $\mu\text{m}$ ) of a triple-grating spectrometer (T64000, Jobin Yvon, Inc.). A polarization analyzer followed by a appropriately oriented  $\lambda/2$  plate between collimator and the entrance slit of the spectrometer were employed to measure the Raman intensity polarized parallel ( $I_x$ ) and perpendicular ( $I_y$ ) to the scattering plane. The scattering light was dispersed by the spectrometer and then detected by a liquid nitrogen cooled charge-coupled device (CCD) with  $256 \times 1024$  pixels in the chip. The spectral resolution was  $4.0 \text{ cm}^{-1}$ . The frequency calibration of the recorded Raman spectra was checked by means of the  $934 \text{ cm}^{-1}$  band of the internal standard, the frequency of which had been determined earlier with high accuracy.<sup>26</sup> For tri-proline the very intense fluorescence background (even after partial quenching by 20  $\mu\text{L}$  of KI)

deteriorated the signal to noise ratio of the Raman spectra. In order to improve the latter, we recorded multiple spectra for both polarization directions and added them up to average the noise. This yielded spectra of sufficient quality for the zwitterionic peptide. For cationic PPP the Raman spectra were further smoothed by averaging a total of ten spectra, which were differently shifted along the wavenumber axis in an interval of  $\pm 5 \text{ cm}^{-1}$ . The thus caused deterioration of spectral resolution could be tolerated in view of the much larger bandwidth of the individual amide I' bands.

**IR Spectroscopy.** FTIR spectra were measured with a Nicolet Magna-IR System 560 optical bench as described elsewhere.<sup>27</sup> A total of 256 scans at  $2 \text{ cm}^{-1}$  resolution using Happ–Ganzel apodization were averaged to obtain each spectrum. For all experiments, a Spectra Tech liquid cell equipped with  $\text{CaF}_2$  windows and  $6\text{-}\mu\text{m}$  thick mylar spacers were used. The peptide sample was put between  $\text{CaF}_2$  windows. Each peptide sample was measured at least four times. Spectra were corrected for the solvent background in an interactive manner using Nicolet OMNIC 3.1 software.

**VCD Spectroscopy.** VCD spectra were measured with a Chiralir FT-VCD spectrometer from Bomem/BioTools, modified to the setup of dual polarization modulation (DPM). The DPM setup includes two ZeSe photoelastic modulators (PEM), one of which is to create left and right circularly polarized radiation and the other is used to suppress the linear birefringence and the associated VCD artifacts. The spectrometer is equipped with a liquid nitrogen cooled HgCdTe detector having a cutoff at  $800 \text{ cm}^{-1}$ . VCD spectra were measured in  $\text{D}_2\text{O}$  with resolution of  $8 \text{ cm}^{-1}$  using a  $\text{CaF}_2$  cell with a pathlength of  $30 \mu$ . The VCD spectra were collected in blocks for a total collection time of approximately 9 h depending on the peptide sample investigated. The VCD spectra of solvent  $\text{D}_2\text{O}$  were also measured at the identical conditions for the purpose of VCD baseline correction and ir spectral solvent subtraction. For all measurements, the PEM was optimized for maximum quarter-wave response at  $1400 \text{ cm}^{-1}$ , which is around the midpoint of spectral range of interest. Other experimental conditions are provided in the figures captions referring to the VCD spectra.

**CD Spectroscopy.** Far-uv CD spectra (250–190 nm) were measured with an OLIS DSM-10 UV/Vis CD spectrophotometer in a 1.0-mm quartz cell with 2 nm resolution. The samples were placed in a nitrogen gas purged OLIS CD module. The temperature at the cuvette was controlled by means of a Peltier-type heating system (accuracy  $\pm 1^\circ\text{C}$ ). For each measurement, the sample in the cuvette was allowed to equilibrate for 5 min at the adjusted temperature prior to data acquisition. For all experiments reported in this article  $\Delta A(\lambda, T)$  was measured by increasing the temperature in increments of  $5^\circ\text{C}$ . The integration time was set as a function of high volts to obtain an appropriate signal-to-noise ratio. The room temperature spectra were obtained by averaging 5 scans. The solvent reference spectra were used

as baselines, which were automatically subtracted from the peptide CD spectra. For the final presentation in this article the original  $\Delta A(\lambda, T)$  spectra were converted to the  $\Delta\epsilon(\lambda, T)$  representation by using the above sample concentrations and the path length of the cuvette.

**Spectral Analysis.** All ir and Raman spectra were analyzed using the program MULTIFIT.<sup>28</sup> They were normalized to the internal standard, i.e., the  $\text{ClO}_4^-$  band at  $934 \text{ cm}^{-1}$ . To eliminate solvent contributions, we measured the solvent reference spectra for both polarizations, which were then subtracted from the corresponding peptide spectra. The intensities of the normalized polarized Raman bands were derived from their band areas. These and the corresponding ir spectrum were self-consistently analyzed in that they were fitted with a set of identical frequencies, halfwidths, and band profiles. The isotropic and anisotropic Raman intensities and the depolarization ratios were calculated as follows:

$$I_{\text{iso}} = I_x - \frac{4}{3}I_y$$

$$I_{\text{ansio}} = I_y \quad (6)$$

$$\rho = \frac{I_x}{I_y}$$

It should be mentioned that in principle  $I_{\text{ansio}}$  should be written as  $8I_y/3$ . As mentioned in earlier articles,<sup>17</sup> we prefer to identify it with  $I_y$  in the depicted figures so that the polarization properties of different lines can be better inferred.

**Density Functional Theorem Calculations.** We used the TITAN program from Wavefunction, Inc., to perform a structural optimization of L-alanyl-L-proline in vacuo with the Becke–Lee–Young–Parr composite exchange functional (B3LYP) at the B3LYP/6-31g level of theory. All harmonic frequencies of the optimized geometry were found to be real, showing that it corresponds to a stable energy minimum.

## RESULTS AND DISCUSSION

### Amide I' of Prolylalanine

As reported in detail below, the Raman spectra of tri-proline (PPP) indicate that the Raman tensor of amide I' depends on the protonation state of the terminal groups, in contrast to what has been found for tri-alanine. This requires a modification of the mathematical algorithm reported in Ref. 23, which is based on the assumption that the amide I' Raman tensors of the two peptide groups are identical. Thus,

in order to fix as many parameters as possible for our analysis, we measured and analyzed the amide I' region of the FTIR as well as of the isotropic and anisotropic Raman spectra of the dipeptide L-prolyl-L-alanine (PA) in D<sub>2</sub>O at acid, neutral, and alkaline pD (Figure 2). In order to allow for comparison, the Raman spectra were normalized by means of the 934 cm<sup>-1</sup> line of sodium perchlorate, which thus served as an internal standard. All ir spectra are displayed as extinction coefficient spectra. The amide I' bands could be satisfactorily fitted by single Voigtian bands

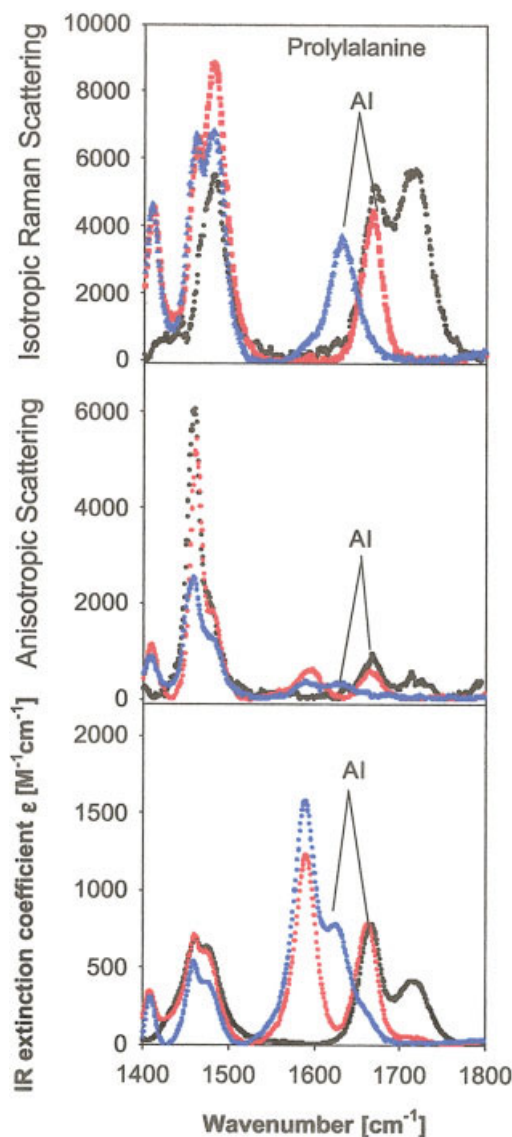


**FIGURE 2** Amide I' region of the FTIR, isotropic, and anisotropic Raman spectra of L-prolyl-L-alanine in D<sub>2</sub>O measured at pD 1 (cationic, black), 6 (zwitterionic, red), and 12 (anionic, blue). The Raman spectra were recorded with 457.9 nm excitation (laser power: 150 mW, slit width: 100 μm).

**Table I** Spectral Parameters and Raman Tensor Elements of the Amide I' Mode of the Three Protonation States of L-Prolyl-L-Alanine

Parameter	Cationic	Zwitterionic	Anionic
$\Omega_{A1}$ (cm <sup>-1</sup> ) <sup>a</sup>	1669	1667	1631
$\Gamma_L$ (cm <sup>-1</sup> ) <sup>b</sup>	10.0	10.0	10.0
$\Gamma_G$ (cm <sup>-1</sup> ) <sup>c</sup>	27	21	29.4
$\rho$	0.14	0.11	0.07
$a^d$	0.65	0.65	0.65
$b^d$	1	1	1
$c^d$	-0.07	-0.07	-0.07
$d^d$	0	0.07	0.25

<sup>a</sup>Wavenumber position.

<sup>b</sup>Lorentzian halfwidth of the Voigtian profile.

<sup>c</sup>Gaussian halfwidth of the Voigtian profile.

<sup>d</sup>Relative tensor elements of the amide I mode.

with the spectral parameters listed in Table I. Small deviations between the fit and experimental profile indicate a slight band asymmetry due to fluctuations of the hydrogen bonds between the peptide and the water molecules in the solvation shell.<sup>29</sup> From the fits we also obtained the integrated band intensities and depolarization ratios listed in Table I. The depolarization ratios of the three protonation states are significantly different, i.e., 0.17, 0.11, and 0.06 for the cationic, zwitterionic, and anionic state of the dipeptide, respectively. This reflects nearly exclusively differences between the anisotropic contribution to the Raman cross section. In contrast, we obtained practically identical ir extinctions for the three protonation states. The obtained variations are in the limit of accuracy. However, a comparison with the ir spectra of di- and tri-alanine revealed a substantial increase of the amide I' oscillator strength by a factor of 3.4. This reflects a 1.8-fold increase of the transition dipole moment. Besides its relevance for our analysis, this result is also important for the ir spectroscopy on peptides and proteins, for which it is generally assumed that the amide I' oscillator strength is independent on the side chain composition.<sup>30</sup>

In order to understand the depolarization ratio we start with the coordinate system visualized in Figure 1. Its *x* axis coincides with the NC<sub>α</sub> bond and its *y* axis lies in the peptide plane to form an angle of 117° with the carbonyl bond. Thus, *z* becomes the out-of-plane coordinate. The peptide nitrogen is chosen as the zero point of the coordinate system. In our earlier studies we assumed that the amide I' intensity reflects vibronic coupling to electronic transitions in the peptide plane (mostly  $\pi \rightarrow \pi_1^*$  (NV<sub>1</sub>) and  $\pi \rightarrow \pi_2^*$  (NV<sub>2</sub>), Figure 3), so that its Raman tensor can be written as<sup>23</sup>:

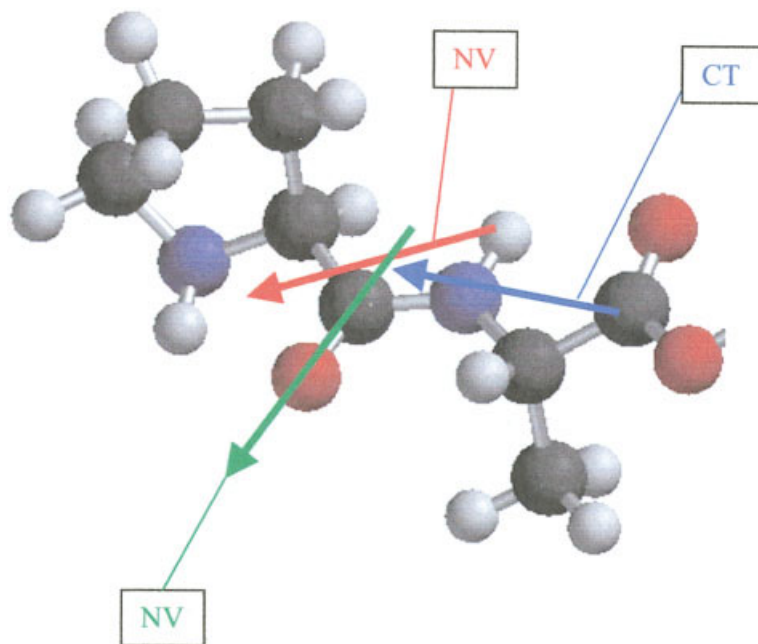


**FIGURE 3** Structure of neutral L-prolyl-L-alanine in vacuo as obtained from the DFT calculation described in the Material and Methods section. The figure also contains the direction of electronic transition dipole moments obtained from Ref. 30. It should be noted that the CT transition occurs only if the C-terminal group is deprotonated.

$$\hat{\alpha} = \begin{pmatrix} a & c & 0 \\ c & b & 0 \\ 0 & 0 & 0 \end{pmatrix} \quad (7)$$

The depolarization ratio varies between 0.75 ( $a=-b$ ) and 0.125 ( $a=b, c=0$ ). The values generally obtained for amide I' with excitation in the visible region are in the range between 0.14 and 0.17, indicating that  $a$  and  $b$  have the same sign and similar values. In order to obtain depolarization values smaller than 0.125 a  $zz$  component has to contribute to the Raman tensor in the PART frame, so that

$$\hat{\alpha} = \begin{pmatrix} a & c & 0 \\ c & b & 0 \\ 0 & 0 & d \end{pmatrix} \quad (8)$$

Now the depolarization ratio can reach the value zero, if  $a=b=d$ . We disregard contributions from  $xz, zx, yz,$  and  $zy$ , since they would all increase rather than decrease the depolarization ratio. One possible candidate for this is the thus far neglected  $n(\text{COO}^-)\leftarrow\pi$  (peptide) charge transfer transition to which amide I' is indeed weakly coupled, since this transition involves expansions of the CO as well as of the CN bond.<sup>31,32</sup> As shown in Ref. 30 for di-glycine the dipole transition moment points from the carboxylate

carbon to the peptide nitrogen (Figure 3). Its orientation with respect to our coordinate system and the PART frame depends on the dihedral angle  $\phi$ . For a PPII conformation ( $\phi=60^\circ\text{--}80^\circ$ ) it would have a substantial  $z$  component, so that vibronic coupling of amide I' to this transition would add a  $zz$  element to the Raman tensor. However, the amide I' Raman tensor obtained for di-glycine crystals by Pajcini et al.<sup>32</sup> suggest that this contribution is very weak with a limited influence on the depolarization ratio. Therefore, we are led to disregard the above charge transfer transition as a possible explanation for the low depolarization values. It must result from vibronic coupling to a yet unidentified electronic transition in the far uv, the dipole moment of which has a substantial  $z$  component. It might be associated with the pyrrolidine ring. A DFT calculation on neutral PA in vacuo (Figure 3) revealed an optimized geometry in which it is nearly perpendicular to the peptide plane. The corresponding  $\psi$  angle ( $165^\circ$ ) is close to the canonical PPII value. We compared the calculated and experimental wavenumbers of the high frequency peptide modes. As expected, the wavenumber of the amide I was substantially overestimated, owing to the neglect of hydrogen bonding to solvent molecules. Since the depolarization ratio of the cationic peptide ( $\rho=0.14$ ) is in the range known from tri-alanine, tri-glycine, and other tripeptides, we assume that the respective Ra-

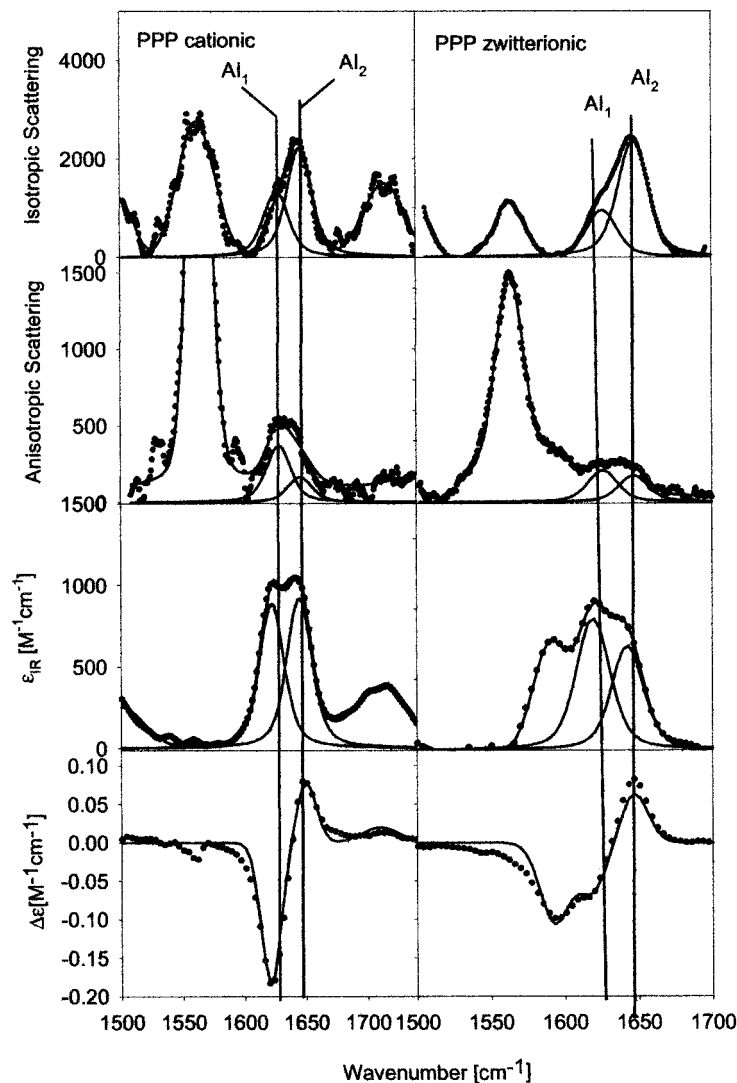


**FIGURE 4** Amide I' region of the FTIR, isotropic Raman, anisotropic Raman, and VCD spectra of L-prolyl-L-prolyl-L-proline in D<sub>2</sub>O measured at pD 1 (cationic) and 7.5 (zwitterionic). The Raman spectra were recorded with 441 nm excitation (laser power: 65 mW, slit width: 100 μm). The line profiles in the IR and Raman spectra result from a global spectral decomposition as described in the Material and Methods section. The solid lines in the VCD spectra result from a calculation based on the dihedral angles obtained from the analysis of the amide band intensities as described in the text.

man tensor of AA has no  $zz$  element and can therefore be described by Eq. (7). Consistency with the diglycine PART tensor obtained by Pajcini et al.<sup>32</sup> it has been shown to require that<sup>23</sup>

$$c = -\frac{b-a}{9.3} \quad (9)$$

The depolarization ratio can be calculated by combining Eqs. (8) and (9) with Eqs. (12), (14), and (15) in Ref. 23. Since it depends on the ratios  $a/b$  and  $c/b$  rather than on the absolute values of the tensor elements, we have to choose an arbitrary value for one of

the tensor elements. In accordance with the findings of Pajcini et al.<sup>32</sup> we identified the  $y$  axis as the major axis of the Raman tensor in the chosen coordinate system and assumed  $b=1$  as a reference value. Thus,  $\rho$  can be reproduced by  $a=0.65$  and  $c=-0.04$ . In the next step, we attributed the somewhat lower depolarization ratio of 0.11 observed for the zwitterionic state to an additional  $zz$  element  $d$  and thus obtained  $d=0.07$ . To account for the even lower depolarization ratio of the anionic peptide,  $d=0.25$  has to be inserted. In the following, we will use the thus derived Raman tensors (listed in Table I) to analyze the amide I' band profile of cationic and zwitterionic PPP.

## Structure Analysis of Tri-Proline

Figure 4 depicts the isotropic Raman, ir, and VCD spectra of the amide I' region of cationic and zwitterionic tri-proline. In a first step, we analyzed the spectra of the zwitterionic peptide, because we obtained the spectra with the best signal to noise ratio for this species. Fluorescence and a lower Raman cross section made the recording of good spectra difficult. The ir and Raman spectra were then analyzed as described under Material and Methods. The obtained intensity ratios  $R_{\text{iso}}$ ,  $R_{\text{aniso}}$ , and  $R_{\text{IR}}$  are listed in Table II. To simulate the  $R_{\text{iso}}$  and  $R_{\text{aniso}}$  as a function of the excitonic mixing parameter  $\nu$ , the orientational angle  $\bar{\theta}$ , and the dihedral angles  $\phi$  and  $\psi$ , we started by using the Raman tensor obtained for anionic and zwitterionic PA for the N and C-terminal amide I', respectively. This did not allow us to reproduce the experimental  $R_{\text{aniso}}$  and the depolarization ratios ( $\rho_- = 0.06$ ,  $\rho_+ = 0.17$ ) because the theoretical orientational dependencies of these parameters were not pronounced enough. Therefore, we allowed for slight changes of the  $d$  values and eventually obtained a satisfactory solution for  $d_{\text{N}} = 0.15$  and  $d_{\text{C}} = 0.1$ , namely the dihedral angles  $\psi = 165^\circ$  and  $\psi = -70^\circ$ . Figure 5 shows  $R_{\text{IR}}$ ,  $R_{\text{aniso}}$ ,  $\rho_-$  and  $\rho_+$  as a function of  $\phi$  for  $\psi = 165^\circ$ . In the limit of accuracy, all experimental values are reproduced in the interval  $\phi = -70^\circ \pm 10^\circ$ . Hence, we obtained nearly the canonical PPII structure from our analysis. We checked for other solutions and found them all in sterically forbidden regions.

The corresponding amide I' VCD signal (Figure 4) was reproduced with the above structural parameters

**Table II** Spectral Parameters of and Geometric Values Derived from the Amide I' Mode of the Three Protonation States of L-Prolyl-L-Prolyl-L-Proline

Parameter	Cationic	Zwitterionic
$\Omega_{AI-}$ ( $\text{cm}^{-1}$ ) <sup>a</sup>	1628	1611
$\Omega_{AI+}$ ( $\text{cm}^{-1}$ ) <sup>a</sup>	1646	1630
$\Gamma_{L-}$ ( $\text{cm}^{-1}$ ) <sup>b</sup>	10.0	10.0
$\Gamma_{L+}$ ( $\text{cm}^{-1}$ ) <sup>b</sup>	10.0	10.0
$\Gamma_{G-}$ ( $\text{cm}^{-1}$ ) <sup>c</sup>	16.9	20.0
$\Gamma_{G+}$ ( $\text{cm}^{-1}$ ) <sup>c</sup>	17.5	23.0
$\rho_-$	0.28	0.11
$\rho_+$	0.08	0.06
$R_{\text{iso}}$	0.37	0.47
$R_{\text{aniso}}$	1.89	0.96
$R_{\text{IR}}$	0.92	1.17
$\bar{\theta}$ ( $^\circ$ )	85	92
$\phi$ ( $^\circ$ )	-80	-60
$\psi$ ( $^\circ$ )	175	150

<sup>a</sup>Wavenumber position.

<sup>b</sup>Lorentzian halfwidth of the Voigtian profile.

<sup>c</sup>Gaussian halfwidth of the Voigtian profile.

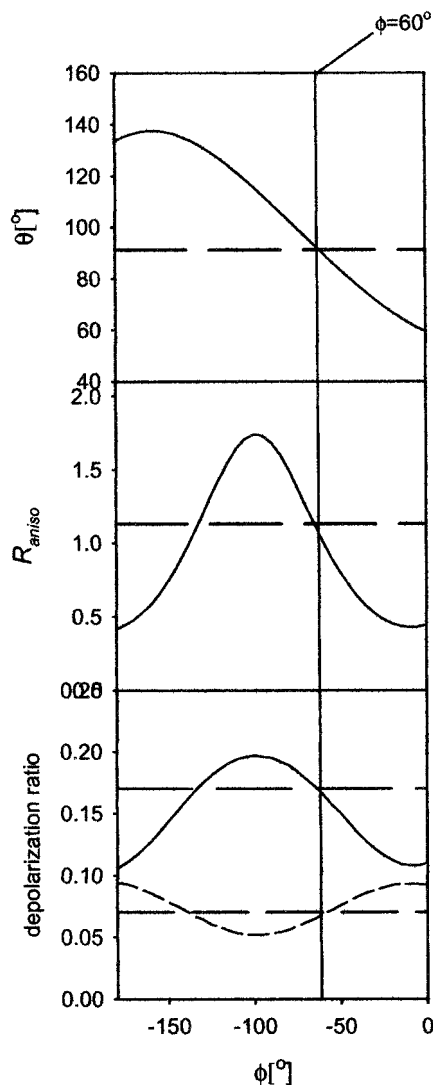


**FIGURE 5** The  $\bar{\theta}$ ,  $R_{\text{aniso}}$ ,  $\rho_-$ , and  $\rho_+$  as function of the dihedral angle  $\phi$  for  $\psi = -165^\circ$  by using the algorithm described in the theory section and the Raman tensors derived in the Results and Discussion section. The horizontal lines depict the respective experimental values. The solid vertical line labels the  $\phi$  values for which all experimental values could be reproduced in the limit of their accuracy.

by considering that the PA ir spectra indicate a much larger dipole transition moment. It should be noted that the negative peak at  $1590 \text{ cm}^{-1}$  results from the  $\text{COO}^-$  antisymmetric stretch. It has been heuristically modeled by a Gaussian profile. We rule out excitonic coupling between this mode and the amide I' of the C-terminal based on the observation that the band of the corresponding  $\text{COO}^-$  is totally depolarized in the Raman spectrum. Excitonic coupling would give rise to some isotropic intensity.

The original Raman spectra of the amide I' region of cationic PPP were very noisy due to a strong

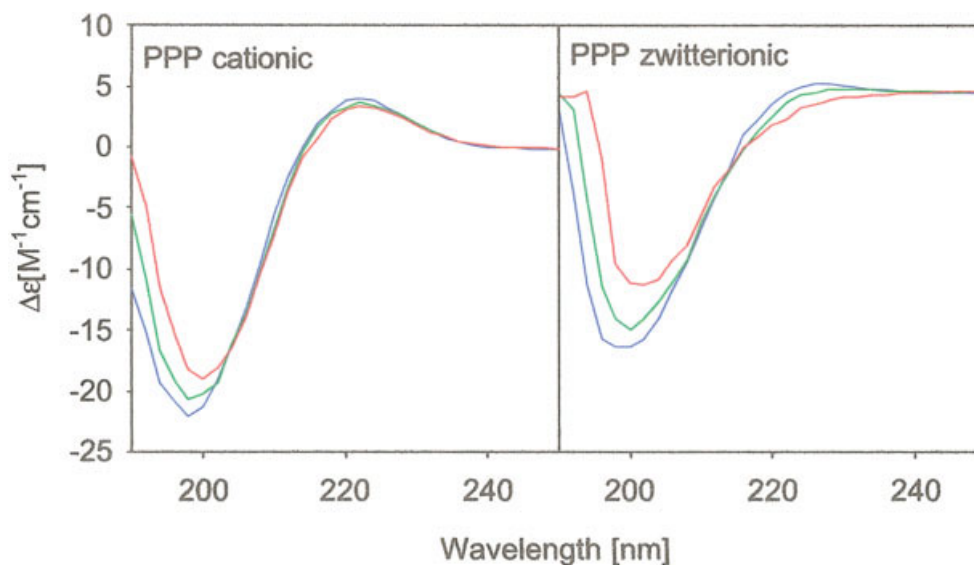


**FIGURE 6** UV-CD spectra of L-prolyl-L-prolyl-L-proline at pD 1 and 7 measured at 20°C (blue), 40°C (green), and 60°C (red).

fluorescence background and a weak relative amide I' intensity. While the spectral averaging described in Material and Methods yielded at least an isotropic spectrum of sufficient quality for the spectral analysis, the eventually obtained anisotropic scattering spectrum must be considered with great caution since it cannot be ruled out that the smoothing procedure has affected the overall band profile. The spectrum displayed in Figure 4 is indicative of a much larger  $R_{\text{aniso}}$  value than that obtained for the zwitterionic species. We believe that this does at least qualitatively reflect the real spectral distribution. It is also theoretically expected owing to the relatively large depolarization ratio observed for cationic PA. We subjected the Raman and ir spectra to a self-consistent analysis, which yielded identical bandwidths but slightly different wavenumber positions for the respective amide I' bands in the ir and Raman spectra. This discrepancy most likely results from the smoothing procedure. The obtained spectral parameters were analyzed as described above to yield  $\psi = 175^\circ + 5^\circ - 15^\circ$  and  $\phi = -80^\circ \pm 20^\circ$ . The relatively large errors reflect the uncertainties of the spectral analysis. This coordinates can still be regarded as reflecting a PPII structure. In the limit of accuracy, one can argue that the central dihedral angles of the zwitterionic and cationic species are identical. We checked the coordinates of the cationic species by calculating the VCD spectrum. In order to account for the asymmetry of the amide I' couplet (Figure 4), we have to assume a magnetic dipole moment for the C-terminal amide I', in accordance with what was obtained for other tripeptides.<sup>14,17</sup> Our calculation yielded a nearly perfect reproduction of the experimental signal.

As a final control of our analysis, we also measured the electronic uv-CD spectra of cationic and zwitterionic PPP. The spectra are shown in Figure 6. For cationic PPP, we obtained a clear and intense PPII signal, which is practically independent on temperature. The variations on the high energy side of the negative signal at 195 nm most likely stem from a temperature dependent overlapping band at lower wavenumbers. The spectra of zwitterionic PPP are in principal similar to that of the cationic species, but are indicative of a weak temperature dependence of the PPII signal. However, that could well result from contributions assignable to the above mentioned charge transfer transition.<sup>31,32</sup> We can therefore conclude that the CD spectra fully confirm the notion that even PPP is locked into a single conformation, which shows a nearly canonical PPII structure. The absence of any significant temperature dependence of the PPII CD signal argues against the presence of additional conformers even at high temperatures. Thus, our results are fully in line with the behavior of longer polyproline peptides investigated by Dukor and Keiderling.<sup>8</sup>

## SUMMARY AND CONCLUSIONS

We have measured and analyzed the amide I' band region in the FTIR and Raman spectra of tri-proline in water. By utilizing a modified version of a recently developed algorithm we were able to determine the dihedral angles between the peptide groups. The thus obtained "secondary" structure of the cationic and zwitterionic peptide is close to the canonical polypro-

line II conformation. Any admixtures from other conformations cannot be inferred from our data. This demonstrates that the preference for this structure is due to local interactions between the pyrrolidine ring and the backbone and not due to any long-range interactions. From this it follows that proline residues should also predominantly (nearly 100%) adopt PPII in proline rich peptides. The PPII contents of a series of AcP<sub>3</sub>XP<sub>3</sub>GY-NH<sub>2</sub> peptides (X represents a set of different residues) reported by Kelly et al. corroborate this notion.<sup>33</sup> For X=P obtained a PPII content of 66%, which one would indeed expect, if one assumes low PPII propensity for G and Y, some reduced stability for the C-terminal P and a nearly 100% PPII occupation for the remaining prolines. In general terms, our study adds another piece of evidence to the notion that tripeptides are ideal tools to understand the so-called random coil state of peptides and proteins.

First of all, we have to thank Dr. Timothy Keiderling from the University of Illinois, Chicago, for strongly suggesting to apply our method to tri-proline. Financial support was provided from the NIH-COBRE II grant for the Center for Research in Protein Structure, Function and Dynamics (P20 RR16439-01), from the NIH-SCORE grant (S06 GM008102-3052) and from the Fondos Institucionales para la Investigación of the University of Puerto Rico (20-02-2-78-514).

## REFERENCES

1. Brant, D. A.; Flory, P. J. *J Am Chem Soc* 1965, 87, 2791–2800.
2. Boicchio, B.; Tamburro, A. M. *Chirality* 2002, 14, 782–792.
3. Shi, Z.; Woody, R. W.; Kallenbach, N. R. *Adv Protein Chem* 2002, 62, 163–240.
4. Cowan, P. M.; McGavin, S. *Nature* 1955, 176, 501–503.
5. Tiffany, M. L.; Krimm, S. *Biopolymers* 1968, 6, 1379–1382.
6. Tiffany, M. L.; Krimm, S. *Biopolymers* 1968, 1767–1770.
7. Paterlini, M. G.; Freedman, T. B.; Nafie, L. A. *Biopolymers* 1986, 25, 1751–1765.
8. Dukor, R.; Keiderling, T. *Biopolymers* 1991, 31, 1747–1761.
9. Seerama, N.; Woody, R. W. *Protein Sci* 2003, 12, 384–388.
10. Siligardi, G.; Drake, A. F. *Biopolymers* 1995, 37, 281–292.
11. Blanch, E. W.; Morozowa-Roche, L. A.; Cochran, D. A. E.; Doig, A. J.; Hecht, L.; Barron, L. D. *J Mol Biol* 2000, 301, 553–563.
12. Han, W. G.; Jalkanen, J.; Elstner, M.; Suhai, S. *J Phys Chem B* 1998, 102, 2587–2602.
13. Weise, C. F.; Weisshaar, J. C. *J Phys Chem B* 2003, 107, 3265–3277.
14. Eker, F.; Cao, X.; Nafie, L.; Huang, Q.; Schweitzer-Stenner, R. *J Phys Chem B* 2003, 107, 358–365.
15. Pappu, R. V.; Rose, G. D. *Protein Sci* 2002, 11, 2437–2455.
16. Dill, K. A. *Protein Sci* 1999, 8, 1166–1180.
17. Eker, F.; Cao, X.; Nafie, L.; Schweitzer-Stenner, R. *J Am Chem Soc* 2002, 124, 14330–14341.
18. Eker, F.; Griebenow, K.; Schweitzer-Stenner, R. *J Am Chem Soc* 2003, 125, 8178–8185.
19. Mu, Y.; Kosov, D. S.; Stock, G. *J Phys Chem B* 2003, 107, 5064–5073.
20. Park, S.-H.; Shalongo, W.; Stellwagen, E. *Protein Sci* 1997, 6, 1694–1700.
21. Shi, Z.; Olson, C. A.; Rose, G. D.; Baldwin, R. L.; Kallenbach, N. R. *Proc Natl Acad Sci USA* 2002, 99, 9190–9195.
22. Helbecque, N.; Loucheux-Lefebvre, M. H. *Int J Peptide Protein Res* 1987, 19, 94–101.
23. Schweitzer-Stenner, R. *Biophys J* 2002, 83, 523–532.
24. Torii, H.; Tasumi, M. *J Raman Spectrosc* 1998, 29, 81–86.
25. Glasoe, P. K.; Long, F. A. *J Phys Chem* 1960, 64, 188–193.
26. Sieler, G.; Schweitzer-Stenner, R. *J Am Chem Soc* 1997, 119, 1720–1726.
27. Griebenow, K.; Diaz Laureano Y.; Santos A. M.; Montañez Clemente I.; Rodriguez L.; Vidal M.; Barletta G. *J Am Chem Soc* 1999, 121, 8157–8163.
28. Jentzen, W.; Unger, E.; Karvounis, G.; Shelnutt, J. A.; Dreybrodt, W.; Schweitzer-Stenner, R. *J Phys Chem* 1996, 100, 14184–14191.
29. Gnanakaran, S.; Hochstrasser, R. M. *J Am Chem Soc* 2001, 123, 12886–12898.
30. Al-Azzam, W.; Pastrana, E.A.; Ferrer, Y.; Huang, Q.; Schweitzer-Stenner, R.; Griebenow, K. *Biophys J* 2002, 83, 3637–3651.
31. Chen, X. G.; Li, P.; Holtz, J. S. W.; Chi, Z.; Pajcini, V.; Asher, S. A.; Kelly, S. A. *J Am Chem Soc* 1996, 118, 9705–9715.
32. Pajcini, V.; Chen, X. G.; Bormett, W.; Geib, S. J. Asher, S. A. *J Am Chem Soc* 1996, 118, 9716–9726.
33. Kelly, M. A.; Chellgreen, B. W.; Rucker, A. L.; Troutman, J. M.; Fried, M. G.; Miller, A.-F.; Creamer, T. P. *Biochemistry* 2001, 40, 14376–14383.